Mechanism of Assembly of the Tyrosyl Radical–Diiron(III) Cofactor of *E. coli* Ribonucleotide Reductase. 2. Kinetics of The Excess Fe^{2+} Reaction by Optical, EPR, and Mössbauer Spectroscopies

J. Martin Bollinger, Jr.,[§,⊥] Wing Hang Tong,[§] Natarajan Ravi,[†,∥] Boi Hahn Huynh,*[,†] Dale E. Edmondson,*[,‡] and JoAnne Stubbe*[,§]

Contribution from the Departments of Chemistry and Biology, Massachusetts Institute of Technology, Cambridge, Massachusetts 02139, and the Departments of Physics and Biochemistry, Emory University, Atlanta, Georgia 30322

Received January 13, 1994®

Abstract: The tyrosyl radical–diiron(III) cofactor of *E. coli* ribonucleotide reductase assembles spontaneously *in vitro* when the iron-free (apo) form of the enzyme's R2 subunit is mixed with Fe^{2+} and O_2. In previous work (Bollinger, J. M., Jr. *et al.*, *Science*, **1991**, *253*, 292–298), kinetic and spectroscopic evidence was presented that the cofactor assembly reaction partitions between two pathways and that the partition ratio depends on the availability of the "extra" reducing equivalent that is required to balance the four-electron reduction of O_2. In this study, stopped-flow absorption, rapid freeze–quench electron paramagnetic resonance, and rapid freeze–quench Mössbauer spectroscopies have been used to examine the kinetics of the reaction carried out with excess Fe^{2+} ($Fe^{2+}/R2 \geq 5.0$). The kinetic data are consistent with a mechanism involving two sequential first-order reactions, in which the diferric radical species, ***X*** (Ravi, N. *et al. J. Am. Chem. Soc.*, previous paper in this issue), accumulates rapidly ($k_{obs} = 5–10\ s^{-1}$) and decays concomitantly with formation of •Y122 and the oxo-bridged diferric cluster ($k_{obs} = 0.7–1.0\ s^{-1}$). The simplest interpretation of these data is that oxidation of Y122 by ***X*** generates the product cofactor and therefore, that Y122 oxidation is not carried out by a high valent iron species. The Mössbauer kinetic data also suggest that a stable or slowly decaying Fe(III)-containing species, which is distinct from the diferric cluster, is produced concomitantly with ***X***. It is proposed that this Fe(III) species may represent the product of donation of the "extra" electron by Fe^{2+}.

Introduction

The ribonucleotide reductases (RNRs) from *E. coli*, mammals, and several medically important viruses (e.g. herpes simplex I and II, and rabies) share a common quaternary structural motif and cofactor requirement.[1–4] Each contains in its R2 subunit a catalytically essential metallocofactor, which consists of a stable tyrosyl radical adjacent to an oxo-bridged diiron(III) cluster. In a reaction which involves reductive activation of O_2 by the diferrous form of the iron cluster, the cofactor assembles spontaneously when apo R2 is treated with Fe^{2+} and O_2.[5,6] Because the cofactor is essential for RNR activity,[5] and because reactions of O_2 at diiron clusters are of general biochemical importance,[7–13] much recent effort has been devoted to elucidating the mechanism by which the R2 cofactor assemblies.[6,14–19]

In our previous work,[14,15] we reported kinetic and spectroscopic evidence for the accumulation of two intermediate species in reconstitution of R2 from *E. coli*. We proposed[14] that the assembly reaction partitions between two distinct pathways (see Scheme 1 of preceding paper[20]) and that a different intermediate iron cluster generates •Y122 in each pathway. The partition ratio between the pathways was postulated to depend on the ratio of Fe^{2+}/apo R2, which was proposed to determine the availability of the "extra" reducing equivalent that is required to balance the four-electron reduction of O_2 (eq 1).[6,16] An earlier report[15] and the preceding paper[20] demonstrate that one of these intermediate species, ***X***, is a spin-coupled cluster consisting of two high-spin ferric ions and a ligand radical.

$$2Fe^{2+} + Y122 + O_2 + 1H^+ + e^- \rightarrow Fe^{3+}\text{–}O^{2-}\text{–}Fe^{3+} + {}^{\bullet}Y122 + H_2O \quad (1)$$

* Authors to whom correspondence should be addressed.
§ Massachusetts Institute of Technology.
† Department of Physics, Emory University.
‡ Department of Biochemistry, Emory University.
⊥ Present address: Department of Biological Chemistry and Molecular Pharmacology, Harvard Medical School, Boston, MA 02115.
∥ Present address: Department of Chemistry, Carnegie Mellon University, Pittsburgh, PA 15213.
® Abstract published in *Advance ACS Abstracts*, August 15, 1994.

(1) Fontecave, M.; Nordlund, P.; Eklund, H.; Reichard, P. *Adv. Enzymol. Rel. Areas Mol. Biol.* **1992**, *65*, 147–183.
(2) Stubbe, J. *Adv. Enzymol. Rel. Areas Mol. Biol.* **1990**, 463, 349–419.
(3) Eriksson, S.; Sjöberg, B.-M. In *Allosteric Enzymes*; Hervé, G., Ed.; CRC Press: Boca Raton, FL, 1989; pp 189–215.
(4) Lammers, M.; Follmann, H. *Struct. Bonding (Berlin)* **1983**, *54*, 27–91.
(5) Atkin, C. L.; Thelander, L.; Reichard, P.; Lang, G. *J. Biol. Chem.* **1973**, *248*, 7464–7472.
(6) Ochiai, E.-I.; Mann, G. J.; Gräslund, A.; Thelander, L. *J. Biol. Chem.* **1990**, *265*, 15758–15761.
(7) Feig, A. L.; Lippard, S. J. *Chem. Rev.* **1994**, *94*, 759–805.
(8) Stubbe, J. *Curr. Opin. Struct. Biol.* **1991**, *1*, 788–795.
(9) Que, L., Jr.; True, A. E. *Prog. Inorg. Chem. Bioinorg. Chem.* **1990**, *38*, 97–200.
(10) Vincent, J. B.; Oliver-Lilley, G. L.; Averill, B. A. *Chem. Rev.* **1990**, *90*, 1447–1467.
(11) Kurtz, D. M., Jr. *Chem. Rev.* **1990**, *90*, 585–606.
(12) Sanders-Loehr, J. In *Iron Carriers and Iron Proteins*; Loehr, T. M., Ed.; VHC Publishers Inc.: Weinheim, 1989; pp 375–466.
(13) Lippard, S. J. *Angew. Chem., Int. Ed. Engl.* **1988**, *27*, 344–361.
(14) Bollinger, J. M., Jr.; Edmondson, D. E.; Huynh, B. H.; Filley, J.; Norton, J. R.; Stubbe, J. *Science* **1991**, *253*, 292–298.
(15) Bollinger, J. M., Jr.; Stubbe, J.; Huynh, B. H.; Edmondson, D. E. *J. Am. Chem. Soc.* **1991**, 4113, 6289–6291.
(16) Elgren, T. E.; Lynch, J. B.; Juarez-Garcia, C.; Münck, E.; Sjöberg, B.-M.; Que, L., Jr. *J. Biol. Chem.* **1991**, *266*, 19265–19268.
(17) Sahlin, M.; Sjöberg, B.-M.; Backes, G.; Loehr, T.; Sanders-Loehr, J. *Biochem. Biophys. Res. Commun.* **1990**, *167*, 813–818.
(18) Fonecase, M.; Gerez, C.; Atta, M.; Jeunet, A. *Biochem. Biophys. Res. Commun.* **1990**, *168*, 659–664.
(19) Ling, J.; Sahlin, M.; Sjöberg, B.-M.; Loehr, T. M.; Sanders-Loehr, J. *J. Biol. Chem.* **1994**, *269*, 5595–5601.
(20) Part 1: Ravi, N.; Bollinger, J. M., Jr.; Huynh, B. H.; Edmondson, D. E.; Stubbe, J. *J. Am. Chem. Soc.*, first of three papers in this issue.

0002-7863/94/1516-8015$04.50/0

Scheme 1. Postulated minimal mechanism for the reaction at 5 °C of apo R2, O_2 and excess Fe^{2+}. The broken circle represents only one of the two monomers of apo R2, and no implication is intended with regard to the chemical identity of the "Fe^{3+}". Modified slightly from reference (14).

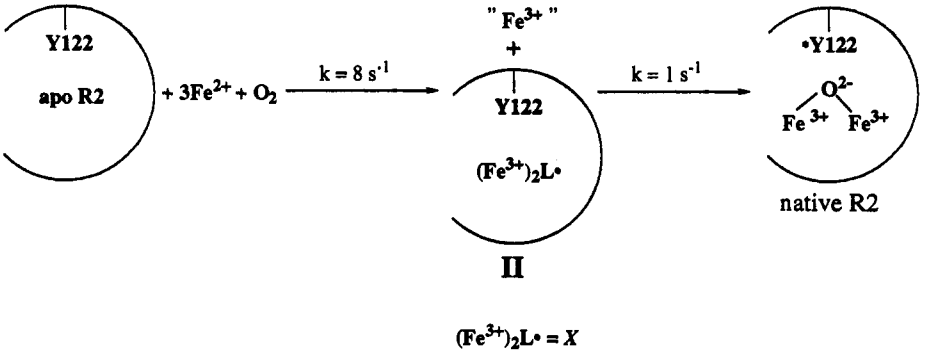

$(Fe^{3+})_2L^{\bullet} = X$

In this paper, we report determination of the Fe^{2+}/•Y122 stoichiometry of the *E. coli* R2 cofactor assembly reaction. The results provide support for two key aspects of our mechanistic hypothesis: (1) that an extra electron is required in the reaction and (2) that both Fe^{2+} and ascorbate are capable of providing this electron. While the requirement for an extra electron and the ability of Fe^{2+} to provide it were previously proposed by Elgren, *et al.* for *E. coli* R2[16] and by Ochiai *et al.* for mouse R2,[6] the conclusions of the two groups regarding the manner in which the electron is delivered were quite different. Our stoichiometry results, when considered with kinetic data which are also presented herein, are more consistent with the conclusions of Ochiai *et al.* Furthermore, the demonstration that alternative reductants such as ascorbate can also deliver the extra electron provides a valuable mechanistic probe which we have exploited in paper 3 of this series.[21]

In the main focus of this work, we have used the complementary kinetic/spectroscopic methods of stopped-flow absorption (SF-Abs), rapid freeze-quench EPR (RFQ-EPR), and rapid freeze-quench Mössbauer (RFG-Möss) spectroscopies to characterize the kinetics of the cofactor assembly with excess Fe^{2+}, under which conditions our previously proposed mechanistic hypothesis (Scheme 1 of the preceding paper)[20] simplifies to Scheme 1, since the extra electron is readily available (from Fe^{2+}) to rapidly convert I into II. By using these methods, rate constants for formation and decay of *X* and for formation of •Y122 and the diferric cluster have been independently measured, and the kinetic constants are in good agreement with those of Scheme 1. The data suggest that *X* generates •Y122 and is the immediate precursor to the product diferric cluster. Thus, the results provide support for our contention that high-valent iron species are not involved in the assembly reaction.[14,15] In addition, the demonstrated consistency of the SF-Abs, RFQ-EPR, and RFQ-Möss data provides the basis for the work described in paper 3 of this series,[21] in which the methods have been used to probe the kinetically and spectroscopically more complex reaction of apo R2 with limiting Fe^{2+}.

Materials and Methods

Materials. Natural abundance (^{56}Fe) iron wire was purchased from Baker (Phillipsburg, NJ). ^{57}Fe was purchased from Advanced Materials and Technology (New York, NY). Ferrozine and the Fe atomic absorption standard were purchased from Sigma (St. Louis, MO). 2-Methylbutane (reagent grade) was purchased from Aldrich (Milwaukee, WI).

Preparation of Apo R2 and Apo R2-Y122F. Detailed procedures for preparation and sequencing of the Y122F mutant *nrd*B gene, for purification of wild-type R2 and R2-Y122F, and for chelation of the iron to produce apo R2 and apo R2-Y122F are given in the supplementary material. Briefly, site-directed mutagenesis was carried out in M13 according to the method of Taylor *et al.*[22] by using a kit from Amersham (Arlington, Heights, IL). DNA sequencing to characterize the mutant *nrd*B gene was carried out by the dideoxynucleotide chain termination method[23] according to the instructions in the U.S. Biochemicals (Cleveland, OH) sequenase kit. Oligonucleotides for mutagenesis and sequencing were synthesized according to the manufacturer's instructions on a Biosearch 8600 DNA synthesizer. The oligonucleotide for mutagenesis was purified by preparative polyacrylamide gel electrophoresis according to a standard procedure.[24] Wild-type protein R2 was isolated from the overproducing strain N6405/pSPS2 as previously reported,[25] with minor modifications. R2-Y122F was overproduced in strain K38, by using the two-plasmid T7 RNA polymerase system of Tabor and Richardson,[26] and was purified by the procedure used for wild-type R2. Apo R2 and apo R2-Y122F were prepared from the respective iron-containing proteins by a previously described chelation procedure.[5,27] For R2-Y122F, the chelation procedure was performed twice in order to ensure complete removal of Fe^{3+} from the protein. Concentrations of apo R2 and apo R2-Y122F were determined by absorbance at 280 nm according to the published molar absorption coefficient (ϵ_{280}) of 120 mM^{-1} cm^{-1}.[28]

Determination of Fe^{2+}/•Y122 Stoichiometry: Titration of Apo R2 with Fe^{2+}. Fe^{2+} stock solutions were prepared by dissolution of $FeSO_4 \cdot 7H_2O$ in anaerobic 0.01 M HNO_3. The concentration of Fe^{2+} ($[Fe^{2+}]$) was determined by a previously described colorimetric procedure which employs the ferroin chelator, ferrozine.[27,29,30] Fe assays were carried out in the absence of ascorbate in order to determine $[Fe^{2+}]$, and with ascorbate present in order to determine total [Fe] ($[Fe^{2+}] + [Fe^{3+}]$).

In a typical titration experiment, 215 μL aliquots of air-saturated 87 μM apo R2 in 100 mM HEPES (pH 7.6) were allowed to reach equilibrium at 5 °C by incubation for approximately 1 h in a cold room. For the titrations with ascorbate, samples were made 4.9 mM in sodium ascorbate immediately prior to addition of Fe^{2+}. An aliquot of a 1.92 mM Fe^{2+} stock was added (such that 0–8 molar equiv of Fe^{2+} relative to apo R2 were delivered) to each sample, with repeated mixing (by inversion) immediately after addition. The samples were incubated for several minutes, and a 20 μL aliquot of each was diluted (for activity assay) to 400 μL with 50 mM HEPES (pH 7.6), containing 20% glycerol. (Glycerol was used to ensure against protein precipitation which can occur upon freezing dilute solutions of R2. The samples for activity assay were stored frozen at −80 °C until the next day, when the assays were carried out.) The specific activity of each of these diluted samples was determined at 25 °C by using the standard coupled assay.[31] The assay mix contained the following in a final volume of 400 μL: 50 mM HEPES (pH 7.6), 15

(21) Part 3: Bollinger, J. M., Jr.; Tong, W. H.; Ravi, N.; Huynh, B. H.; Edmondson, D. E.; Stubbe, J. *J. Am. Chem. Soc.*, third of three papers in this issue.

(22) Taylor, J. W.; Ott, J.; Eckstein, F. *Nucleic Acids Res.* **1985**, *13*, 8765–8785.
(23) Sanger, F.; Nicklen, S.; Coulson, A. R. *Proc. Natl. Acad. Sci. U.S.A.* **1977**, *82*, 5463–5467.
(24) Sambrook, J.; Fritsch, E. F.; Maniatis, T. *Molecular Cloning: A Laboratory Manual*; 2nd ed.; Cold Spring Harbor Laboratory Press: Cold Spring Harbor, 1989; Vol. 1.
(25) Salowe, S. P.; Stubbe, J. *J. Bacteriol.* **1986**, *165*, 363–366.
(26) Tabor, S.; Richardson, C. *Proc. Natl. Acad. Sci. U.S.A.* **1985**, *82*, 1074–1078.
(27) Salowe, S. P. Ph.D. Thesis, University of Wisconsin, 1987.
(28) Thelander, L. *J. Biol. Chem.* **1973**, *248*, 4591–4601.
(29) Stookey, L. L. *Anal. Chem.* **1970**, *42*, 779–781.
(30) Massey, V. *J. Biol. Chem.* **1957**, *229*, 763–770.
(31) Mao, S. S.; Holler, T. P.; Yu, G.-X.; Bollinger, J. M., Jr.; Booker, S.; Johnston, M. I.; Stubbe, J. *Biochemistry* **1992**, *31*, 9733–9743.

mM $MgSO_4$, 1 mM EDTA, 1.5 mM ATP, 0.16 mM NADPH, 1.0 mM CDP, 0.5–2.0 μg of R2, 30 μg of R1, 50 μg of thioredoxin, and 3 μg of thioredoxin reductase. Each concentrated sample was diluted with 215 μL of 40% glycerol in H_2O (again, to ensure that the protein would not precipitate when it was frozen for EPR spectroscopy) and a UV–visible absorption spectrum of each was recorded at 5 °C. A 400 μL aliquot of each sample was transferred to an EPR tube and then frozen in liquid N_2. An EPR spectrum of each was acquired at 100 K on a Brüker ESP 300 spectrometer equipped with a Brüker ER4111VT variable temperature controller. The concentration of tyrosyl radical in each sample was determined by double integration of the first derivative spectrum and comparison of the double integral to those of three different concentration standards. The first standard contained 0.973 mM $CuSO_4$, 2 M $NaClO_4$, 0.01 M HCl, and 20% (v/v) glycerol.[32] The second contained 0.343 mM $CuSO_4$ and 3.4 mM EDTA.[33] The third contained 134 μM $K_2(SO_3)_2$-NO in 50 mM HEPES buffer (pH 7.6) with 20% glycerol.[34] For the R2 samples and the Cu^{2+} standards, the microwave power was 1 mW, and for the $K_2(SO_3)_2NO$ standard the power was 3.1 μW. (It was verified that the signals were not saturated at these powers.) Other EPR parameters include the following: microwave frequency, 9.38 GHz; modulation amplitude, 4 G; modulation frequency, 100 kHz; scan time, 160 s; time constant, 1 ms; receiver gain, 5×10^4. Double integrals of samples and standards were corrected for difference in the *g* value, as previously described.[35] After correction for *g*-value differences, all three EPR spin concentration standards agreed to within 3%.

Preparation of Stock Solutions for SF-Abs, RFQ-EPR, and RFQ-Mössbauer Experiments. Fe^{2+} stock solutions for the kinetics experiments were prepared by dissolution at 60 °C of ^{56}Fe or ^{57}Fe metal in O_2-free 1 M H_2SO_4. The volume of H_2SO_4 added was such that 4 molar equiv of H^+ relative to Fe^0 were initially present. Upon complete dissolution (which took 12–24 h) the Fe^{2+} stock was assumed to contain 2 mol of H^+ per mol of Fe^{2+}, since H_2 is evolved in conversion of Fe^0 to Fe^{2+}. This stock was diluted either with H_2O or with dilute H_2SO_4, in order to give the desired concentration of Fe^{2+} in 4–6 mM H^+. The concentration of Fe^{2+} was verified by the ferrozine assay.[27,29,30]

Kinetics of the Reaction of Apo R2 with Excess Fe^{2+} and O_2 Monitored by SF-Abs, RFQ-EPR, and RFQ-Mössbauer. In order to ensure that O_2 was in excess in the kinetics experiments, both the apo R2 stock solution and the Fe^{2+} stock solution were saturated with 1 atm of O_2 (giving $[O_2]$ after mixing >1 mM[36]) prior to their being loaded into the stopped-flow or rapid freeze-quench syringes. In each experiment, 0.55–0.64 mM apo R2 in O_2-saturated 100 mM HEPES (pH 7.7) was mixed at 5 °C with an equal volume of O_2-saturated $^{56}Fe^{2+}$ or $^{57}Fe^{2+}$ stock solution. The concentration of Fe^{2+} in the stock solution was such that the Fe^{2+}/R2 ratio was 4.9–5.1.

Unless otherwise noted, SF-Abs experiments were carried out on an Applied Photophysics (Leatherhead, UK) DX.17MV sequential stopped-flow spectrofluorimeter. The temperature was maintained at 5 °C with a Lauda K-2/R ciculating water bath (Brinkmann Instuments). The water in the bath was purged with pure O_2 throughout all experiments as a precaution against diffusion of dissolved air (which would deplete the dissolved O_2) through the polytetrafluoroethylene flow lines.

RFQ-EPR samples were prepared as previously described.[37,38] The apparatus used is described in the preceding paper.[20] EPR spectra were acquired on a Brüker ER 200D-SRC spectrometer equipped with an Oxford Instruments ESR 910 continuous flow cryostat. Unless otherwise indicated, the spectra were recorded at 20 K with a microwave power of 2 μW, a frequency of 9.43 GHz, a modulation frequency of 100 kHz, a modulation amplitude of 4 G, a time constant of 200 ms, a scan time of 200 s, and a receiver gain of 4×10^4.

Analysis of the EPR spectra of the time-course samples to determine the relative quantities of ***X*** and •Y122 present in each was carried out with a subtraction program written by B.H.H. The 60 s time-point of the reaction was used as a reference spectrum for •Y122. A freeze-quenched sample from the reaction of apo R2-Y122F with excess Fe^{2+} was used as a reference sample for ***X***. In the preparation of this sample, 0.14 mM apo R2-Y122F in argon-saturated 100 mM HEPES (pH 7.7), was mixed at 5 °C with an equal volume of 1.0 mM Fe^{2+} in air-saturated 5 mM HNO_3 and the reaction was quenched at 0.27 s. By manual iteration, the reference spectra of ***X*** and •Y122 were summed in varying ratios until the experimental spectrum of each time-course sample was satisfactorily reproduced. In the calculation of the absolute concentrations of the two species, the 60 s sample was used as a standard. The •Y122/R2 ratio upon completion of the reaction was known to be 1.2 ± 0.1 from the stoichiometry experiments and from the SF-Abs experiments.

RFQ-Mössbauer samples were prepared as described in the preceding paper.[20] All Mössbauer spectra were acquired at 4.2 K with a magnetic field of 50 mT applied parallel to the γ-beam. In order to determine the quantities of the various iron species present in each of the freeze-quenched samples, experimental spectra were deconvoluted into component spectra by iterative application of a subtraction program written by R. Zimmermann. For each of the three components, ferrous-R2, ***X***, and the diferric cluster, both experimental and theoretical spectra were used as references for analysis of the time-course spectra. Experimental spectra for ferrous-R2 and for the diferric cluster were acquired on samples which are described below. Theoretical spectra for these components were generated either by non-linear least-squares fitting of two quadrupole doublets to the data or by simulation (using parameters from the least-squares fit or from Lynch *et al.*[39]). For ***X***, the theoretical spectrum from the preceding paper[20] was used as a reference for quantitation of the intermediate. Because the central region of this spectrum shows imperfect agreement with the experimental spectrum, when an objective of the analysis was to subtract away the spectrum of ***X*** in order to identify other components of the reaction, it was necessary to use an experimental spectrum as the reference so as not to distort the central region of the subtraction spectrum. The spectrum of Figure 3A from the preceding paper[20] was used as the experimental reference for ***X***. Approximately 70% of the integrated intensity of this spectrum is contributed by ***X***, with the remainder being contributed predominantly by ferrous-R2 or by ferrous ions in solution. Therefore, before this spectrum was used as a reference, the contribution from Fe^{2+} was first subtracted away.

Non-linear regression analysis on the EPR and Mössbauer kinetic data was carried out with the Git and Gear programs of Drs. R. J. McKinney and F. J. Wiegert, Central Research and Development Department, E. I. du Pont de Nemours and Co.

Preparation of Mössbauer Reference Samples. Reference samples for ferrous-R2 were prepared by mixing apo R2 in O_2-free 100 mM HEPES (pH 7.7) with either 2.5 or 5.0 molar equiv of $^{57}Fe^{2+}$ in O_2-free 5 mM H_2SO_4 and then freezing the samples in Mössbauer cells. Final concentrations for these samples were 0.66 mM apo R2, 1.66 mM $^{57}Fe^{2+}$ and 0.50 mM apo R2, 2.5 mM $^{57}Fe^{2+}$, respectively. A reference sample for the diferric cluster of R2 was prepared by mixing 0.14 mL of 4.4 mM $^{57}Fe^{2+}$ in 4.5 mM H_2SO_4 containing 14 mM ascorbic acid with 0.25 mL of 0.98 mM apo R2 in air-saturated 100 mM HEPES (pH 7.7) and incubating the solution on ice (open to air) for 45 min prior to freezing it in a Mössbauer cell. A reference sample for $^{57}Fe^{2+}$ in HEPES buffer was prepared by mixing (at 5 °C) equal volumes of O_2-saturated 100 mM HEPES buffered at pH 7.7 with O_2-saturated 1.5 mM $^{57}Fe^{2+}$ stock and freeze-quenching the mixture after 0.44 s.

Control to Show Equivalence of Mössbauer Samples and EPR Samples. As described in the preceding paper,[20] the apparatus and procedure developed for preparation of RFQ-Mössbauer samples require somewhat more manipulation after quenching than those used in preparation of EPR samples. In order to verify that quantitative comparison of data for the two types of samples would be meaningful, it was deemed essential to ensure that the slightly different methods of preparation generate identical samples. Therefore, a control was performed in which a Mössbauer sample was prepared in the usual manner and was subsequently transferred and repacked into an EPR tube. (Both transfer and repacking were carried out under cold isopentane.) A second sample was prepared under identical reaction conditions but was quenched and packed in the usual manner for preparation of EPR samples. EPR spectra at 20 K of the two samples were acquired and were found to be identical.

Results

Determination of Fe^{2+}/•Y122 Stoichiometry. In order to determine the Fe^{2+}/•Y122 stoichiometry of the reconstitution reaction, Fe^{2+} was added in varying molar ratios to aliquots of air-saturated apo R2, and the quantity of •Y122 produced was

(32) Malmström, B.; Reinhammar, B.; Vänngård, T. *Biochem. Biophys. Acta* **1970**, *205*, 48.
(33) Broman, L.; Malmström, B.; Aasa, R.; Vänngård, T. *J. Mol. Biol.* **1962**, *5*, 301.
(34) Jones, M. T. *J. Chem. Phys.* **1963**, *38*, 2892–2895.
(35) Aasa, R.; Vänngård, T. *J. Magn. Reson.* **1975**, *19*, 308–315.
(36) Hitchman, M. L. *Measurement of Dissolved Oxygen*; Wiley: New York, 1978.
(37) Ballou, D. P.; Palmer, G. *Anal. Chem.* **1974**, *46*, 1248.
(38) Bray, R. C. *Biochem. J.* **1961**, *81*, 189.
(39) Lynch, J. B.; Juarez-García, C.; Münck, E.; Que, L., Jr. *J. Biol. Chem.* **1989**, *264*, 8091–8096.

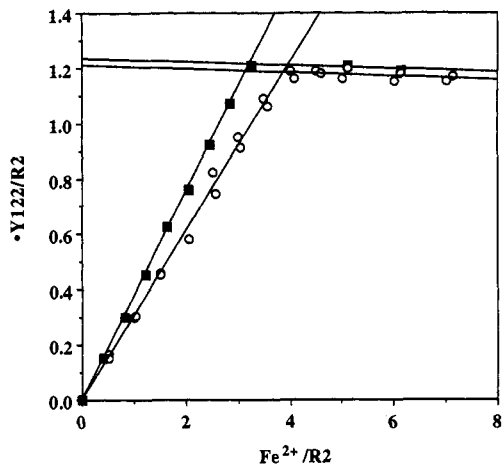

Figure 1. EPR quantitation of •Y122 produced as a function of Fe^{2+} added in reconstitution of R2 in the absence (circles) and in the presence (squares) of ascrobate. The experimental protocol is described in the Materials and Methods section.

determined by EPR spectroscopy. The titrations were carried out in the presence and in the absence of the reductant ascorbate and were also monitored by absorption spectroscopy and by enzymatic activity assay. When Fe^{2+} is added to an air-saturated solution of apo R2 in the absence or in the presence of ascorbate, the R2 cofactor is rapidly formed. The tyrosyl radical content as determined by EPR increases proportionally to the quantity of Fe^{2+} added, until a critical ratio of Fe^{2+}/R2 is reached, at which point no additional •Y122 is produced (Figure 1). The absorbance at 410 nm (due to •Y122) and the specific enzyme activity exhibit identical dependence on the quantity of Fe^{2+} added (data not shown). In the absence of ascorbate, the Fe^{2+}/R2 ratio required for complete reconstitution is 4.0 ± 0.1 and the •Y122/R2 ratio is 1.2 ± 0.1. From these values, a Fe^{2+}/•Y122 stoichiometry of 3.3 ± 0.3 is calculated. This ratio suggests that Fe^{2+} provides the fourth electron under these conditions.

When the titration is carried out in the presence of 4.9 mM sodium ascorbate, the Fe^{2+} ratio at completion is 3.1 ± 0.1 and the •Y122/R2 ratio is 1.2 ± 0.1. From these values, a Fe^{2+}/•Y122 stoichiometry of 2.6 ± 0.3 is calculated. Because this ratio is significantly less than that observed in the absence of ascorbate, and significantly less than the theoretical stoichiometry were ascorbate not to participate in the reaction ($3Fe^{2+}$/•Y122), the data suggest that ascorbate can also provide the fourth electron. The observed stoichiometry is significantly greater, however, than the theoretical lower limit ($2\ Fe^{2+}$/•Y122). As we have previously suggested,[14] this discrepancy could reflect competition between ascorbate and Y122 for reduction of the •Y122-generating intermediate.

A Spectrophotometric Method for •Y122 Quantitation. The numerous samples generated in these titration experiments made it possible to develop a spectrophotometric method to quantify •Y122. The absorption band with λ_{max} = 410 nm, which arises from •Y122, is much sharper than any other spectral feature of R2. When the absorbance at 410 nm of a sample of R2 is corrected to the line defined by the absorbance at 404 nm and the absorbance at 416 nm, only the sharp feature of the tyrosyl radical contributes, since the broader features are well approximated as straight lines over this 12 nm wavelength range. Thus, this "dropline corrected" absorbance at 410 nm ($A_{410,dropline}$) should be directly proportional to [•Y122], irrespective of the conditions under which the R2 is reconstituted. This proportionality was verified by plotting $A_{410,dropline}$ versus [•Y122] (as determined by EPR) for the >80 samples which were generated in titration experiments such as those described above. The slope of this plot gave the proportionality constant ($\epsilon_{410,dropline}$) as 2.11 ± 0.05 $mM^{-1}\ cm^{-1}$.[40] With $\epsilon_{410,dropline}$ determined, [•Y122] could readily be calculated from the absorption spectrum of an R2 sample.

Scheme 2. Kinetic Model Used in Analysis of SF-Abs, RFQ-EPR, and RFQ-Mössbauer Kinetic Data[a]

$$A \xrightarrow{k_1} X \xrightarrow{k_2} Fe^{3+}\text{-}O^{2-}\text{-}Fe^{3+} + \bullet Y122$$

[a] Species A represents the reactants (apo R2, Fe^{2+}, and O_2) and *X* is the diferric radical species.

Reaction of Apo R2 with Excess Fe^{2+} and O_2 Monitored by SF-Abs. We previously reported the time-dependent absorption spectra of the reaction at 5 °C of apo R2 with excess Fe^{2+} and O_2.[14] Under the conditions which were employed, development of the spectrum of the cofactor is complete within 30 s and is characterized by the rapid appearance of a broad band centered near 360 nm, followed by the slower formation of the 390 and 410 nm features of •Y122 and the 320 nm and 365 nm features of the diferric cluster. The results were interpreted as evidence for the mechanism of Scheme 1, with the 360 nm band ascribed to the intermediate iron cluster, *X*. These SF-Abs experiments were carried out at concentrations (<60 μM R2) too low to permit application of the RFQ-Mössbauer method. In the present work, it was deemed essential to carry out the SF and RFQ kinetics experiments under the same set of reaction conditions, in order to allow for direct comparison of the results and as a precaution against concentration-dependent effects. Therefore, the SF-Abs experiments were repeated at reactant concentrations (300 μM R2) suitable for Mössbauer spectroscopy. The same characteristics in development of the cofactor spectrum are observed at these higher concentrations. A broad shoulder at 360 nm develops rapidly, followed by development of the bands due to •Y122 and the diferric cluster.

To test their consistency with the mechanism of Scheme 1, time-dependent absorption spectra from experiments carried out both at high (290–300 μM) and at low (20–60 μM, previously reported[14]) R2 concentrations were analyzed in two ways. First, $A_{410,dropline}$ was used to determine the quantity of •Y122 formed as a function of reaction time. A representative trace is shown in Figure 2. The time-course of •Y122 formation exhibits no dependence on R2 concentration. The magnitude of $A_{410,dropline}$ at completion observed in five separate experiments (with multiple shots taken in each experiment) is consistent with a •Y122/R2 ratio of 1.2 ± 0.1, in agreement with the titration experiments. More importantly, as Figure 2 demonstrates, formation of •Y122 exhibits a lag phase. A lag is expected from the mechanism of Scheme 1, due to intervention of the intermediate **II** between the reactants (Fe^{2+} and apo R2) and the product (native R2, which contains •Y122). To evaluate whether the $A_{410,dropline}$-versus-time traces are consistent with the kinetic constants of Scheme 1, the 0–5 s regions of several such traces were analyzed according to eq 2, which give $A_{410,dropline}$ as a function of time ($A_{410,dropline}(t)$) for the kinetic sequence of Scheme 2 (assuming that both A and *X* have $\epsilon_{410,dropline} = 0$). $A_{410,dropline}(t)$ is related to the concentration of •Y122 at completion ([•Y122]$_\infty$), the dropline-corrected molar absorptivity at 410 nm of •Y122 ($\epsilon_{410,dropline}$), and the rate constants k_1 and k_2. A representative fit from this analysis is shown in Figure 2. The data are consistent with a rate constant (k_1) of 4.9–7.5 s^{-1} for formation of the intermediate and a rate constant (k_2) of 0.72–0.77 s^{-1} for formation of •Y122.

(40) In the course of carrying out the stoichiometry experiments, it was discovered that $\epsilon_{410,dropline}$, and indeed the entire UV–visible absorption spectrum of R2, exhibits a significant dependence on temperature. The spectra used to calculate the reported value of $\epsilon_{410,dropline}$ were acquired at 5 °C. For experiments carried out at temperatures other than 5 °C, it was necessary to correct $\epsilon_{410,dropline}$ appropriately. It should also be noted that, due to the sharpness of this absorption feature, $\epsilon_{410,dropline}$ is dependent on the spectral resolution and on the wavelength calibration of the spectrophotometer used. Therefore, it was also necessary to determine $\epsilon_{410,dropline}$ separately for each spectrophotometer used.

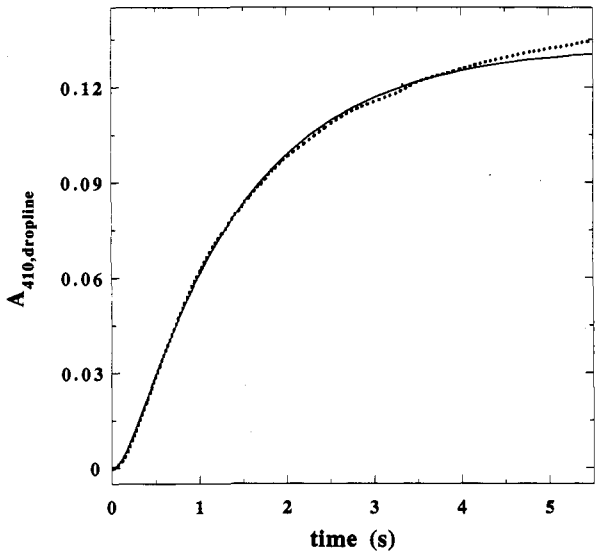

Figure 2. Representative $A_{410,dropline}$-versus-time trace to assess the time-course of •Y122 formation in the reaction of apo R2 with excess Fe^{2+}. The reaction conditions were the following: 0.295 mM R2, 1.45 mM Fe^{2+}, 50 mM HEPES (O_2-saturated), pH 7.6, 5 °C. The experimental trace (dotted line) was constructed as $A_{410} - (A_{404} + A_{416})/2$ by averaging three trials for each wavelength. The theoretical curve (solid line) is a least-square fit according to eq 2, with k_1 = 6.4 s^{-1}, k_2 = 0.75 s^{-1}, and $[•Y122]_\infty \epsilon_{410,dropline}$ = 0.133.

These values for k_1 and k_2 are in satisfactory agreement with those of Scheme 1. Analysis of the time-dependent absorption spectra by a multicomponent analysis protocol (Applied Photophysics Global Analysis) also gave rate constants in satisfactory agreement with those of Scheme 1 (k_1 = 3.9 s^{-1}, k_2 = 0.49 s^{-1}).

$$A_{410,dropline}(t) = [•Y122]_\infty \epsilon_{410,dropline}\left(1 + \frac{k_1 \exp(-k_2 t) - k_2 \exp(-k_1 t)}{k_2 - k_1}\right) \quad (2)$$

Reaction of Apo R2 with Excess Fe^{2+} Monitored by RFQ-EPR. In our previous work we demonstrated that reaction of apo R2 with excess Fe^{2+} and O_2 leads to the rapid formation of an EPR active intermediate, ***X***, which is characterized by a sharp, isotropic, g = 2.00 singlet.[14] ***X***, which we have subsequently demonstrated to consist of two high-spin ferric ions coupled to a ligand radical,[15,20] decays concomitantly with formation of •Y122. These results were interpreted as evidence for Scheme 1, though no quantitative analysis of the spectra was attempted. Like the previously reported SF-Abs studies, these experiments were carried out at reactant concentrations (50 μM R2) too low to be useful in RFQ-Mössbauer experiments. The EPR time-course was therefore repeated with higher reactant concentrations (300 μM R2). Development of the EPR spectrum is identical at these higher concentrations (data not shown).

In addition to the aforementioned results with wild-type R2 (R2-wt), we previously demonstrated that the sharp, isotropic, g = 2.00 singlet characteristic of ***X*** also rapidly develops when apo R2-Y122F is mixed in the presence of O_2 with excess Fe^{2+}.[15] In contrast to the R2-wt reaction, the line shape of the spectrum in the g = 2 region does not change with time in the reaction of the mutant protein. This result suggests that, in the absence of the oxidizable Y122, ***X*** is the only EPR active component (with g = 2) which accumulates in the excess Fe^{2+} reaction. Therefore, the R2-Y122F reaction provides a reference EPR spectrum for ***X*** (see Figure 6A of the preceding paper[20]) which can be used to estimate the relative amounts of ***X*** and •Y122 present in the time-course samples from the R2-wt reaction. The relative quantities of the two species were estimated for each time-point by iterative addition of the spectra of ***X*** and •Y122, in varying ratios, until the experimental spectrum was satisfactorily reproduced. At all times during the reaction the spectrum can be accounted for as the sum of the spectra of ***X*** and •Y122. Figure 3 shows representative examples of this analysis. By using the 60 s sample as a radical concentration standard (•Y122/R2 at completion = 1.2), the absolute quantities of ***X*** and of •Y122 (in terms of molar equivalents relative to R2) in each sample were calculated according to eqs 3 and 4, where $I(t)$ is the double integral for a given sample, $F_X(t)$ and $F_{•Y122}(t)$ are the fractions of ***X*** and •Y122 present in that sample, and $I(60)$ is the double integral for the 60 s sample. The quantities of ***X***/R2 and •Y122/R2 as functions of time were analyzed according to the kinetic model of Scheme 2. A rate constant (k_1) of 10 s^{-1} for formation of ***X*** and a rate constant (k_2) of 0.95 s^{-1} for its decay and the concomitant formation of •Y122 were obtained (Figure 4). The concentrations of ***X*** and •Y122 as functions of time suggest, in agreement with Scheme 1, that decay of ***X*** and formation of •Y122 are concomitant processes.[41] This result is consistent with the interpretation that ***X*** generates •Y122.

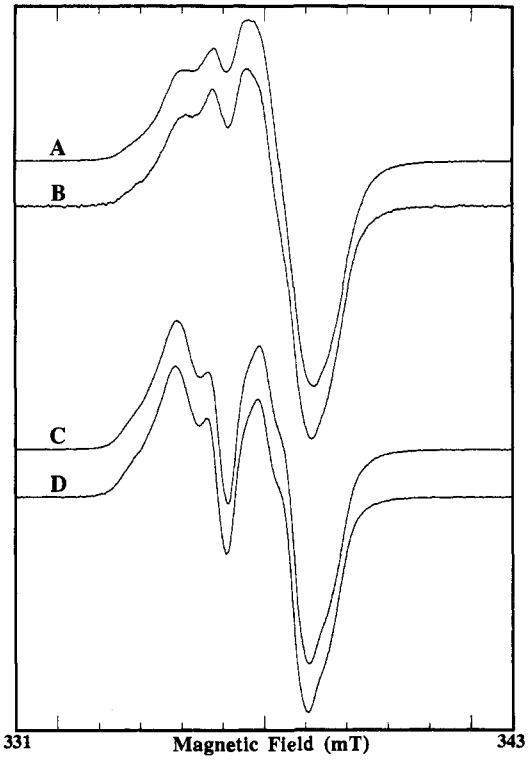

Figure 3. Representative analyses of RFQ-EPR spectra to determine relative quantities of ***X*** and •Y122. Spectrum A was acquired on the 0.44 s sample, and B was constructed by summation of the spectra of ***X*** and •Y122 in a ratio of 0.67:0.33. Spectrum C was acquired on the 1.5 s sample, and D was constructed by summation of the spectra of ***X*** and •Y122 in a ratio of 028:0.72. The spectrum of the 60 s time-point was taken as the reference for •Y122. Preparation of the reference sample for ***X*** is described in the Materials and Methods section.

$$X/R2 = 1.2 \times F_X(t) \times I(t)/I(60) \quad (3)$$

$$•Y122/R2 = 1.2 \times F_{•Y122}(t) \times I(t)/I(60) \quad (4)$$

Reaction of Apo R2 with Excess Fe^{2+} Monitored by RFQ-Mössbauer. The successful characterization of ***X*** by RFQ-Mössbauer[15,20] suggested that the method might be used to investigate the reconstitution kinetics. In principle, Mössbauer spectroscopy

(41) As shown in Figure 4, formation of •Y122 as monitored by RFQ-EPR does not exhibit the lag phase predicted by Scheme 1. This observation contrasts with the clear lag phase in •Y122 production detected by SF-Abs. The reason for this discrepancy is not known, but speculation regarding possible explanations has been presented.[42]

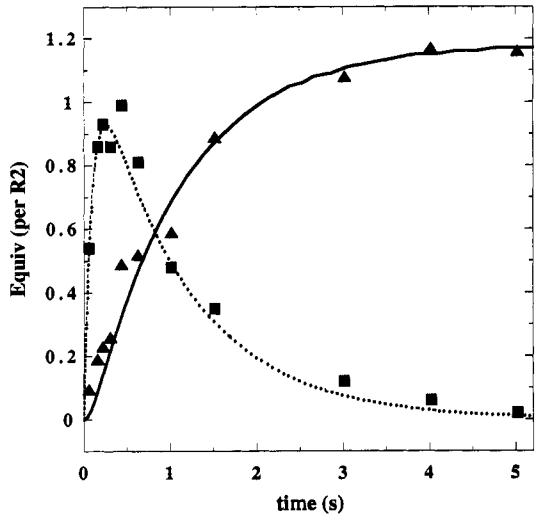

Figure 4. Non-linear least-squares analysis of quantities of X (squares) and •Y122 (triangles) (as determined by RFQ-EPR) as functions of time. The equations appropriate for the kinetic model of Scheme 2 were fit to the data. The solid and dotted lines represent the best fit, with k_1 = 10 s^{-1}, k_2 = 0.95 s^{-1}, and $(•Y122/R2)_{final}$ = 1.2.

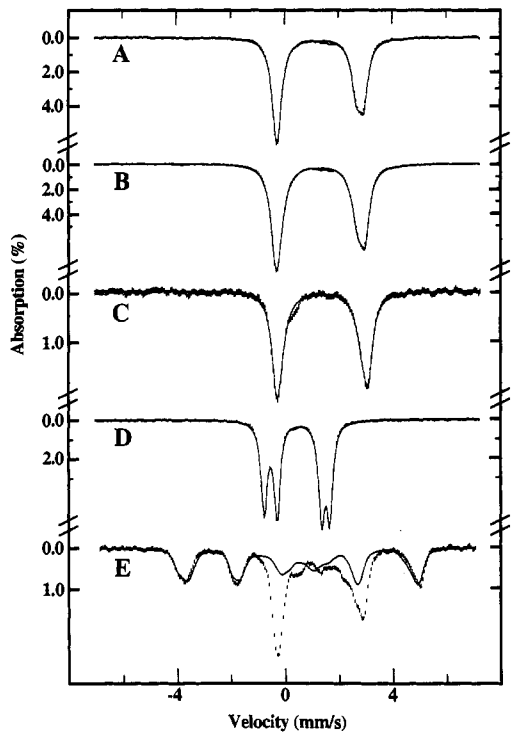

Figure 5. Reference Mössbauer spectra for apo R2 + 2.5 equiv of Fe^{2+} (A), apo R2 + 5.0 equiv of Fe^{2+} (B), Fe^{2+} in HEPES (C), the diferric cluster (D), and the diferric radical species (E). Preparation of spectra A–D is described in the Materials and Methods section. The solid lines through the data are least-squares fits to two quadrupole doublets. Preparation of E is described in the preceding paper.[20] The solid line is a simulation from our previous study.[15] The parameters used for Fe site 2 in this simulation are slightly different from those given in Table 1. The differences do not affect quantitation of the species.

allows all iron-containing species present in a given sample to be quantified simultaneously, provided experimental spectra can be deconvoluted as superpositions of appropriate reference spectra. Figure 5 shows reference spectra for ferrous-R2 (A and B), ferrous ions in HEPES (C), the diferric cluster (D), and X (E). Mössbauer parameters for these species are listed in Table 1.

With the spectra of Figure 5 as references, RFQ-Möss was used to monitor the time-course of the excess Fe^{2+} reaction under conditions identical with those used in the SF-Abs and RFQ-

Table 1. Mössbauer Parameters for Fe(II)-R2,Fe^{2+} in HEPES, the Diferric Cluster, and the Diferric Radical Species (X)

species	site	ΔE_Q (mm/s)	δ (mm/s)	η	$\lvert A/g_n\beta_n\rvert$ (T)
ferrous-R2	1	3.24 ± 0.06[a]	1.31 ± 0.03[a]		
	2	2.92 ± 0.06[a]	1.20 ± 0.03[a]		
		(3.13)[b]	(1.26)[b]		
ferrous ion in	1	3.39 ± 0.06[a]	1.40 ± 0.003[a]		
HEPES buffer	2	3.03 ± 0.06[a]	1.36 ± 0.03[a]		
diferric	1	1.64 ± 0.04[a]	0.54 ± 0.02[a]		
		(1.62 ± 0.02)[c]	(0.55 ± 0.01)[c]		
	2	2.41 ± 0.04[a]	0.45 ± 0.02[a]		
		(2.44 ± 0.03)[c]	(0.45 ± 0.01)[c]		
diferric–	1	−1.0	0.55	0.5	−52.5
radical (X)[d]	2	−1.0	0.36	1.0	+24.0

[a] Obtained by a least-squares fit of two quadrupole doublets to the data. [b] Average of parameters quoted in ref 39. [c] Parameters quoted in ref 39. [d] Parameters from the best simulation in the preceding paper.[20]

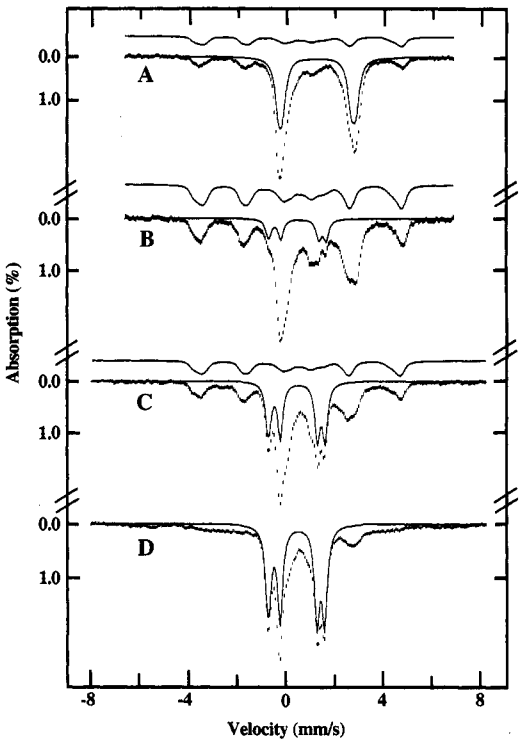

Figure 6. Time-dependent Mössbauer spectra of the reaction of apo R2 with excess Fe^{2+}. The reaction was quenched (A) at 0.061, (B) 0.31, (C) 1.0, or (D) 60 s. The solid line plotted over the data in A is a simulation of the ferrous-R2 spectrum which was obtained by using the parameters reported by Lynch *et al.*[39] It is scaled to 45% of the integrated intensity of the experimental spectrum. The solid line plotted just above the data in A is the theoretical spectrum of X scaled to 20% of the intensity of the experimental spectrum. In B and C, the solid line above the data is the theoretical spectrum of X (36% in B and 23% in C), and the line plotted over the data is the theoretical spectrum of the diferric cluster (12% in B and 32% in C). The solid line in D is the theoretical spectrum of the diferric cluster (55%). The diferric cluster reference spectrum is a simulation based on the values of ΔE_Q and δ from the least-squares fit of Figure 5D (see Table 1).

EPR experiments. The time-dependent spectra clearly reflect the progress of the reaction. In the first time-point taken (0.061 s, Figure 6A), the spectrum is dominated by unreacted ferrous ion. At the first time-point, a significant quantity of X has accumulated, while the features of the diferric cluster are not yet detectable. At somewhat longer reaction times (0.31 s, Figure 6B), the relative quantity of Fe^{2+} present has decreased significantly, while the contribution due to X has increased. In addition, the spectrum of the diferric cluster is now detectable. With increasing reaction time (1.0 s, Figure 6C), the relative contributions from Fe^{2+} and from X decrease, while that from the diferric cluster increases. Finally, at completion of the reaction

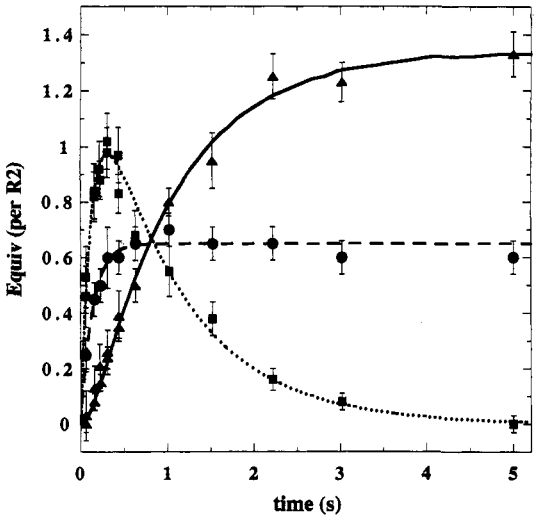

Figure 7. Quantities of *X* (squares), diferric cluster (triangles), and putative fast-relaxing ferric species (circles) as functions of time, as determined by analysis of the RFQ-Mössbauer spectra. The solid and dotted lines are fits (according to Scheme 2) to the data for the diferric cluster and *X*, respectively. They correspond to $k_1 = 7.3\ s^{-1}$, $k_2 = 1.03\ s^{-1}$, and diferric cluster/R2 at completion = 1.34. The dashed line is a simple first-order fit to the data for the fast-relaxing ferric species. It corresponds to $k = 7.3\ s^{-1}$ and fast-relaxing ferric species/R2 at completion = 0.65.

(60 s, Figure 6D), the spectrum is dominated by the features of the diferric cluster.

In addition to illustrating the progress of the reaction, Figure 6 also shows that both *X* and the diferric cluster can be quantified as functions of time from the Mössbauer spectra. The highest and two lowest energy lines of *X* are well-resolved from other spectral features.[20] Likewise, for the diferric cluster, both lines of the outer quadrupole doublet (site 2 in Table 1) are sufficiently resolved from other spectral features to allow for reliable quantitation (see Figure 6 parts B–D). By using these resolved features, the quantities of *X* and the diferric cluster in each time-point were estimated as described in the Materials and Methods section. The quantity of *X* as a function of time exhibits the expected rise–fall behavior, while the quantity of the diferric cluster rises smoothly (Figure 7). The ratio of diferric cluster per R2 subunit at completion (1.38 ± 0.08) is in reasonable agreement with the Fe content of native R2 as determined in our laboratory[42] (2.8–3.2 Fe/R2 assuming $\epsilon_{280} = 131\ mM^{-1}\ cm^{-1}$).[28] The ratio also is only slightly different from the •Y122/R2 ratio (1.2 ± 0.1) observed upon completion of the reaction.

The equations for the kinetic model of Scheme 2 were fit to the measured quantities of *X* and differic cluster as functions of time (Figure 7). The data are consistent with this simple model. The analysis gives a rate constant (k_1) of 7.3 ± 1 s^{-1} for formation of *X* and a rate constant (k_2) of 1.0 ± 0.1 s^{-1} for decay of *X* and concomitant formation of the diferric cluster. The results suggest, in agreement with Scheme 1, that *X* is the immediate precursor to the diferric cluster.

In addition to the obvious features of ferrous-R2, the diferric-radical intermediate (*X*), and the diferric cluster, several other features can be discerned in the time-dependent Mössbauer spectra. Perhaps the most informative of these is a resolved peak centered at approximately 1 mm/s, just slightly lower in energy than the high-energy line of site 1 of the diferric cluster spectrum (Figure 8A). This peak develops rapidly and is therefore prominent in the early time-points of the reaction (0.061–0.63 s), before it becomes obscured by the features of the diferric cluster. The peak does not develop when the reaction is carried out with limiting Fe^{2+} (Figure 8B), nor when the reaction is carried out in the presence of ascorbate (data not shown). The peak also does not develop when Fe^{2+} is mixed with HEPES buffer in the absence of apo R2 (Figure 5C).

(42) Bollinger, J. M., Jr. Ph.D. Thesis, Massachusetts Institute of Technology, 1993.

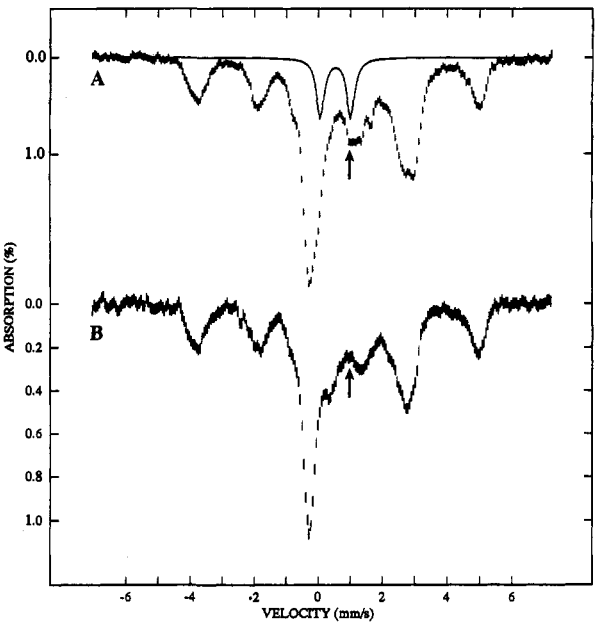

Figure 8. RFQ-Mössbauer spectra showing that a resolved peak at ~1 mm/s develops rapidly only in the excess Fe^{2+} reaction. Spectrum A is the 0.31 s time-point of the excess Fe^{2+} reaction. The solid line over the data is the hypothetical reference spectrum for the fast-relaxing ferric species scaled to 10% of the integrated intensity of the experimental spectrum. It is a simulation based on the parameters given in the text. Spectrum B is the 0.28 s time-point of the limiting Fe^{2+} reaction (see the following paper[21]). It was prepared by mixing (at 5 °C) 0.59 mM apo R2-wt in O_2-saturated 100 mM HEPES (pH 7.7) with an equal volume of 1.34 mM $^{57}Fe^{2+}$ in O_2-saturated 2.5 mM H_2SO_4. The arrow shows where the feature of the fast-relaxing ferric species would be.

Because only one of an unknown number of spectral features associated with the species is resolved, definitive determination of its oxidation and spin state is not possible. Nevertheless, analysis of the spectra of all the time-points is consistent with the interpretation that the resolved peak is the high-energy line of a quadrupole doublet. The low-energy line is obscured in the spectra of early time-points by the low-energy line of the ferrous ion spectrum. In spectra of later time-points, both lines of the doublet can be discerned as apparent shoulders inside the two inner lines of the diferric cluster spectrum (Figure 6D). The parameters ($\delta = 0.56$ and $\Delta E_Q = 0.95$) determined for this species indicate that it contains high-spin ferric ion. The simulated spectrum is shown in Figure 8A (solid line). The lack of magnetic hyperfine splitting in its spectrum suggests either that the electronic relaxation of the ferric ion is rapid compared to that of the nuclear precession frequency or that the ferric ion is in a diamagnetic cluster. Strong magnetic field spectra (data not shown) suggest that the former explanation is correct, and we have therefore tentatively assigned the resolved peak to a fast-relaxing ferric species.

By using the solid line of Figure 8A as a reference spectrum for this putative fast-relaxing ferric species, the species was quantified as a function of time in the same manner as were X and the diferric cluster. The species accumulates rapidly to 0.6–0.7 equiv of Fe(III) per R2 subunit (approximately one-half the quantity of diferric cluster present upon completion) and then decays very slowly (if at all) during the reaction (Figure 7). Analyzing these data according to the equation for a first-order growth gives a formation rate constant of 7.3 ± 1.5 s^{-1}. Thus, the putative fast-relaxing ferric species accumulates with a rate constant identical with that for formation of *X*. Equivalent rate constants for formation of *X* and the fast-relaxing ferric species

have also been observed in the excess Fe^{2+} reaction of R2-Y122F, in which case both processes are slower by a factor of 2.[43] A possible implication of these results is that the putative fast-relaxing ferric species is produced (in one-half of the total events) when Fe^{2+} donates the extra electron which is required for formation of ***X***.

Discussion

Reaction Stoichiometry. An essential step in studying any reaction mechanism is determination of the stoichiometry of reactants and products. Initial efforts of several groups investigating the R2 cofactor assembly were directed toward this objective.[6,14,16] Ochiai *et al.* measured the Fe^{2+}/tyrosyl radical stoichiometry (3.4 ± 0.3) for reconstitution of R2 from mouse.[6] In a more extensive study, Elgren *et al.* determined the Fe^{2+}/•Y122 (3.9 ± 0.5) and O_2/•Y122 (1.3 ± 0.2) ratios for reconstitution of R2 from *E. coli*.[16] As indicated, both groups measured Fe^{2+}/tyrosyl radical stoichiometries in excess of 3. Recognizing that an "extra" electron (in addition to the three provided by oxidation of Y122 and the diferrous cluster) is required to balance the four-electron reduction of O_2 (eq 1), both groups concluded that oxidation of a third Fe^{2+} ion provides this extra electron. On the basis of EPR detection of "mononuclear" Fe^{3+} as a product of the reaction, Ochiai *et al.* proposed that a third Fe^{2+}-binding site exists in mouse R2 to deliver this electron.[6] In contrast, Elgren *et al.* proposed (on the bases of the Fe^{2+}/•Y122 and O_2/•Y122 stoichiometries and Mössbauer characterization of the reconstituted R2 product) that Fe(II) bound in the cluster-binding site of one monomer donates the extra electron to the assembling cluster in a different monomer and that the resulting Fe(II), Fe(III) cluster reacts (in a complex manner) to yield the diferric cluster.[16]

Consistent with the above studies, the Fe^{2+}/•Y122 stoichiometry which we have measured (3.3 ± 0.3) indicates that Fe^{2+} provides the extra electron in the absence of other reductants. However, while our value is within the sum of errors of that determined by Elgren *et al.*,[16] it is inconsistent with the detailed electron-counting model put forth by these authors, which predicts a Fe^{2+}/•Y122 ratio of 4.[44] Moreover, in both the titration and kinetics experiments, our •Y122/R2 ratio at completion (1.2 ± 0.1) is significantly greater than 1 and is only slightly less than the diferric cluster/R2 ratio (1.38 ± 0.08) determined in the RFQ-Möss experiments. Both of these results are inconsistent with the model of Elgren *et al.*, which predicts •Y122/R2 and diferric cluster/R2 ratios of 1 and 2, respectively. More convincingly, the observation that the kinetics of formation and decay of ***X*** and of formation of the diferric cluster are extremely well fit according to Scheme 2 is irreconcilable with the model of Elgren *et al.*, in which diferric cluster is generated in multiple steps, of which only one would be expected to involve reduction of ***X***. Thus, under the reaction conditions which we have employed, the detailed electron counting model of these authors[44] appears to be inaccurate. Our results, especially the detection by RFQ-Möss of the putative fast-relaxing ferric species (discussed in detail below), are more consistent with the conclusion of Ochiai *et al.*[6] for mouse R2 that the Fe^{3+} produced in delivery of the extra electron is not incorporated into a diferric cluster, though we cannot rule out a partition among different fates.

Kinetics and Mechanism of the Excess Fe^{2+} Reaction. In order to test the mechanistic hypothesis of Scheme 1, the complementary methods of SF-Abs, RFQ-EPR, and RFQ-Möss were used to thoroughly characterize the kinetic behavior of the reaction at 5 °C of apo R2, excess Fe^{2+}, and O_2. Acquired under identical reaction conditions, data from each of the three methods provide independent evidence that the diferric-radical species, ***X***, is kinetically competent to oxidize Y122 by one electron to yield •Y122 and the product diferric cluster. The time-courses of formation and decay of ***X*** and of formation of •Y122 as determined by RFQ-EPR are well modeled by assuming that ***X*** generates •Y122. Likewise, the kinetics of formation and decay of ***X*** and of formation of the diferric cluster as measured by RFQ-Möss are consistent with the hypothesis that ***X*** is the precursor to the diferric cluster. The rate constants calculated from the two methods imply that formation of •Y122 and the diferric cluster are concomitant processes. Finally, analysis of the SF-Abs data gives rate constants in agreement with those determined by the RFQ methods, thus providing continuous data in support of the discontinuous RFQ results. The demonstrated consistency of results from the two types of experiments is crucial to the subsequent paper in this series, in which SF-Abs and RFQ data are compared to gain significant insight into the kinetically and spectroscopically more complex reaction of apo R2 with limiting Fe^{2+}.[21]

Scheme 1, which accounts for all the kinetic and spectroscopic data in terms of two sequential, first-order processes, represents the least complex mechanism that can accommodate the data. Clearly the first process in this minimal mechanism, formation of intermediate **II** from apo R2, Fe^{2+}, and O_2, is composed of several steps: binding of Fe^{2+} by apo R2, binding of O_2 by the Fe(II)–R2 complex, and chemical steps (including delivery of the extra electron) which result in formation of ***X***. At least two of these steps, Fe^{2+} and O_2 binding, would be expected to exhibit non-zero kinetic orders in the relevant reactant concentrations. Thus, it is somewhat surprising and quite informative that the reaction kinetics are completely independent of the absolute concentrations of apo R2, Fe^{2+}, and O_2. Invariant kinetic behavior was observed in SF-Abs experiments in which the R2 concentration varied from 25 to 300 μM. At a given R2 concentration, increasing the Fe^{2+}/R2 ratio from 5 to 10 also had no discernable effect.[42] In addition, experiments in which the reactant solutions were air-saturated (giving an O_2 concentration of ~0.3 mM) gave data that were identical with those obtained when both solutions were O_2-saturated (giving an O_2 concentration in excess of 1 mM). These results imply that formation of **II** is of kinetic order zero in both [Fe^{2+}] and [O_2], which implies that the rate determining step in formation of **II** cannot be the bimolecular association of Fe^{2+} and apo R2 or of O_2 and ferrous–R2. Two other possibilities exist for the nature of this step. A slow conformational change in apo R2 may be required to allow for Fe^{2+} and/or O_2 binding. Alternatively, a slow chemical step may occur subsequent to Fe^{2+} and O_2 binding. In the latter scenario, an intermediate R2–Fe_2–O_2 species would accumulate, and such a species would be expected to exhibit visible absorption features. It is therefore more likely that a conformational change in apo R2 limits the rate of formation of **II**. This deduction is consistent with the X-ray crystallographic finding[45,46] that no obvious channel exists in R2 to allow entry of Fe^{2+} and O_2 into the buried cluster-binding site. It also raises the possibility that formation of **II** upon reaction of the pre-formed Fe(II)–R2 complex with O_2 might be significantly faster if the inferred conformational change is required for Fe^{2+} binding but not for O_2 binding. This possibility is being tested.

As discussed above, a central feature of the reconstitution reaction which must be accounted for in any mechanistic hypothesis is the requirement for an extra electron. The stoichiometry results of Ochiai *et al.*[6] and Elgren *et al.*[16] and those reported in this work all indicate that oxidation of a third Fe^{2+} ion provides the extra electron when no other reductant is present. Moreover, our kinetic and spectroscopic results indicate that the extra electron is delivered to the assembling cluster prior

(43) Tong, W. H.; Ravi, N.; Huynh, B. H.; Edmondson, D. E.; Stubbe, J., unpublished observations.

(44) It is possible that differences in experimental protocol account for the discrepancies among our results and those of Elgren et al. For example, our experiments were carried out at 5 °C while their's were conducted at 25 °C.

(45) Nordlund, P.; Sjöberg, B. M.; Eklund, H. *Nature* **1990**, *345*, 593–598.

(46) Norlund, P.; Eklund, H. *J. Mol. Biol.* **1993**, *232*, 123–164.

to or during formation of the diferric radical species: ***X*** is oxidized by just one electron relative to the diferric cluster, and it obtains this electron by oxidizing Y122. Taken together, these results imply that 1 equiv of Fe^{3+} must be formed per equiv of ***X*** produced (see Scheme 1). The stoichiometry results[6,16] suggest three possibilities for the chemical identity of this Fe^{3+} ion. Elgren *et al.* proposed that it is part of a transient Fe(II), Fe(III) cluster, which is converted to the diferric cluster.[16] Conversely, Ochiai *et al.* proposed that the Fe^{3+} is bound in mononuclear fashion at a site distinct from the cluster site.[6] On the basis of these two studies, one might expect the extra Fe^{3+} to exist in a mixed valent (ferrous, ferric) cluster, a diferric cluster, a mononuclear species, or some combination of the three. The putative fast-relaxing ferric species observed in this study accumulates to 0.6–0.7 equiv and with a rate constant identical with that at which ***X*** forms. These kinetic data suggest that the fast-relaxing ferric species might represent the Fe^{3+} which is produced when Fe^{2+} donates the extra electron during formation of ***X***. The species does not, however, account for all of the required extra electrons. If it is assumed that all of the diferric cluster which is produced (1.38 ± 0.08 equiv) results from reduction of ***X***, then the maximum quantity of the fast-relaxing ferric species (0.65 equiv) accounts for slightly less than half of the total quantity of ***X*** produced. Moreover, throughout the reaction the quantity of fast-relaxing Fe(III) is approximately one-half the sum of the quantities of ***X*** and diferric cluster present at that time. For example, at 0.061 s, 0.5 equiv of ***X*** has formed while only 0.25 equiv of fast-relaxing ferric species has been produced. At this time, essentially no diferric cluster is present, so the product cluster cannot account for the missing electrons.

Since the fast-relaxing ferric species accounts for only one-half of the extra electrons required, it would appear reasonable that an additional ferric-containing species might be present. In attempting to detect such an Fe^{3+} species, we observed that the Mössbauer spectra of the later time-points have magnetic features which are resolved outside the highest and lowest energy lines of ***X*** (Figure 6D). It is tempting to speculate that these magnetic features might arise from an R2-bound Fe(II), Fe(III), proposed by Elgren *et al.* to be an intermediate in the reaction.[16] A ferromagnetically coupled ($S = {}^9/_2$) Fe(II), Fe(III) form of R2 has recently been produced (in low yield) and characterized by Hendrich *et al.*[47] A cluster with this large value of S would be expected to exhibit large magnetic splitting. If the magnetic features seen in our spectra are due to a ferromagnetically-coupled Fe(II), Fe(III) cluster, the quantitation of this cluster would account for the additional 0.7 equiv (relative to R2) of electrons required for formation of 1.3–1.4 equiv of ***X***. However, our attempts to observe the EPR signal reported for the $S = {}^9/_2$ cluster have thus far failed. Nevertheless, the features are paramagnetic in nature and may arise from an Fe(III)-containing species, which may ultimately account for the remaining 0.7 equiv of extra electrons.

In summary, the complementary SF-Abs, RFQ-EPR, and RFQ-Mössbauer kinetic data presented herein are consistent with the proposal that the diferric radical species, ***X***, generates •Y122 and is the immediate precursor to the diferric cluster in the reaction of *E. coli* apo R2 with O_2 and excess Fe^{2+}. As the preceding paper demonstrates that ***X*** does not contain Fe(IV),[20] it appears likely that high-valent iron species are not responsible for •Y122 generation under these reaction conditions.

Acknowledgment. This work was supported by NIH Grant GM 29595 to J.S. with a supplemental grant to D.E.E. and B.H.H. and by a Whitaker Health Sciences Foundation Fellowship to J.M.B.

Supplementary Material Available: Detailed procedures for preparation and sequencing of the Y112F mutant *nrd*B gene, purification of wild type R2 and R2-Y122F, and chelation of iron to produce apo R2 and apo R2-Y122F and tables giving the quantities of ***X*** and •Y122 determined by RFQ-EPR and ***X***, the diferric cluster, and the putative fast-relaxing ferric species determined by RFQ-Mössbauer spectra (8 pages). This material is contained in many libraries on microfiche, immediately follows this article in the microfilm version of the journal, and can be ordered from the ACS; see any current masthead page for ordering information.

(47) Hendrich, M. P.; Elgren, T. E.; Que, L., Jr. *Biochem. Biophys. Res. Commun.* **1991**, *176*, 705–710.